

RSC Advances



This article can be cited before page numbers have been issued, to do this please use: P. Liu, G. Li, W. Chang, M. Wu, Y. Li and J. Wang, *RSC Adv.*, 2015, DOI: 10.1039/C5RA12243K.



This is an *Accepted Manuscript*, which has been through the Royal Society of Chemistry peer review process and has been accepted for publication.

Accepted Manuscripts are published online shortly after acceptance, before technical editing, formatting and proof reading. Using this free service, authors can make their results available to the community, in citable form, before we publish the edited article. This *Accepted Manuscript* will be replaced by the edited, formatted and paginated article as soon as this is available.

You can find more information about *Accepted Manuscripts* in the [Information for Authors](#).

Please note that technical editing may introduce minor changes to the text and/or graphics, which may alter content. The journal's standard [Terms & Conditions](#) and the [Ethical guidelines](#) still apply. In no event shall the Royal Society of Chemistry be held responsible for any errors or omissions in this *Accepted Manuscript* or any consequences arising from the use of any information it contains.

Cite this: DOI: 10.1039/c0xx00000x

www.rsc.org/xxxxxx

ARTICLE TYPE

Highly dispersed Pd nanoparticles supported on nitrogen-doped graphene with enhanced hydrogenation activity

Ping Liu,^{*a} Gen Li,^a Wan-Ting Chang,^a Meng-Yao Wu,^a Yong-Xin Li^{*a} and Jun Wang^b*Received (in XXX, XXX) Xth XXXXXXXXX 20XX, Accepted Xth XXXXXXXXX 20XX*

DOI: 10.1039/b000000x

Pd nanoparticles supported on nitrogen-doped graphene (NG) were prepared as hydrogenation catalysts. Different nitrogen sources (ethylenediamine, ammonia, and urea) were employed to synthesise NG by hydrothermal treatment at a mild condition. The as-made samples were characterized by transmission electron microscopy, scanning electron microscopy, Raman spectroscopy, elemental analysis, nitrogen adsorption-desorption, X-ray diffraction, and X-ray photoelectron spectroscopy. Remarkably improved dispersion of Pd nanoparticles were observed when nitrogen was introduced into the graphene structure. These NG-supported Pd catalysts showed enhanced catalytic hydrogenation activities owing to the superior dispersion of Pd. In the hydrogenation of different olefins, perfect turnover frequencies were obtained over NG-supported Pd catalyst with urea as the nitrogen source.

1. Introduction

Metals, especially noble metals Pt, Pd, Rh, and Au, loaded on the support are widely used as catalysts in catalytic hydrogenation reactions because of their high activity, superior stability and reusability.¹ As for the supported catalysts, the properties of supports would greatly influence the catalytic performances from different perspectives such as the state of metal nanoparticles, the adsorption and/or diffusion of reactant and products.^{2,3} Generally, an ideal support should promote the dispersion of metals and accelerate the diffusion of reactant and products. Although many supports (e.g. Al_2O_3 ,⁴ SiO_2 ,⁵ activated carbon,⁶ zeolite,⁷ SBA-15⁸ and carbon nanotube (CNTs)⁹) have been studied during the past few decades years, the researchers never stop seeking the new materials to further improve the activity of loaded metal catalysts.

As an emerging member of carbon materials family, graphene with a unique two-dimensional (2D) honeycomb lattice structure shows unusual properties, including excellent electrical and thermal conductivity, extraordinary thermal and mechanical stability, and extremely high theoretical specific surface area (theoretical $2620 \text{ m}^2 \cdot \text{g}^{-1}$).^{10,11} These properties make graphene to be a potential ideal support for loading metal nanoparticles.^{12,13} However, in the process of loading metal catalyst on the graphene, some issues are exposed such as the uneven dispersion of metal active sites, and loss and/or aggregation of metal nanoparticles due to the relatively weak interaction between graphene and metal.¹⁴ In order to solve these problems, some surfactants,¹⁵ ligands,¹⁴ and polymers¹⁶ have been applied to stabilize the nanoparticles. Unfortunately, these additives are usually expensive and may severely restrict the catalytic activities. In comparison, nitrogen doping into the framework of

carbon materials is more effective to anchor metal nanoparticles depending on the interaction between N species and metal nanoparticles.¹⁷⁻²⁰ Significantly, nitrogen doping also introduces structural defects and alters the electronic structure of graphene, which may promote the catalytic process.²¹

Some methods have been reported to synthesize nitrogen-doped graphene (NG), such as chemical vapour deposition,²² thermal annealing graphene oxide with NH_3 ,²³ arc discharge,²⁴ and hydrothermal method.²¹ The first three methods all require rigorous conditions or special instruments. Hydrothermal treatment is deemed to be a facile and low-cost process to prepare NG. Recently, Yu et al.²⁵ developed a hydrothermal reaction to synthesize NG with graphene oxide and organic amine as precursors at a much low temperature. The obtained NG showed a remarkably enhanced performance for ultrafast supercapacitor. Nevertheless, it has not been studied about whether the NG synthesized by the facile hydrothermal method can be used as an effective support to highly disperse the metal nanoparticles and further improve the catalytic activity.

To circumvent this problem, in this work, we synthesize NG with different nitrogen sources through hydrothermal process, and use the NG as support to load Pd nanoparticles. Influences of the properties of NG on the state of Pd particles and the catalytic hydrogenation performances are in detail investigated.

2. Experimental

2.1 Preparation of catalysts

2.1.1 Synthesis of NG

Graphene oxide (GO) was prepared via ultrasonic exfoliating the graphite oxide obtained by the modified Hummer's method.²⁶ NG was synthesized through a facile hydrothermal method using GO

as the precursor. In a typical process, nitrogen source (ethylenediamine, ammonia, or urea) was gradually added into 40 mL of GO suspension ($2 \text{ mg} \cdot \text{mL}^{-1}$) in deionized water. The mixture was stirred at room temperature for 10 min and subsequently moved to a 50-mL Teflon-lined autoclave. After hydrothermal treatment at $180 \text{ }^\circ\text{C}$ for 12 h, the mixture was naturally cooled to room temperature, and the product was obtained by centrifugation, followed by washing with deionized water and drying in vacuum. The prepared NG was denoted as NG- x - y , x indicates the nitrogen source (EDA: ethylenediamine, AW: ammonia, Urea: urea) and y indicates the micromolar quantity of the input of nitrogen element.

2.1.2 Synthesis of Pd/NG

40 mg NG, 0.2 mL PdCl_2 aqueous solution ($0.02 \text{ mol} \cdot \text{L}^{-1}$), and 40 mL deionized water were added into a round-bottom flask. After mixing uniformly, 1 mL hydrazine hydrate was then dropwise added with magnetically stirring for 30 min. Subsequently, the mixture was centrifuged, and the obtained solid catalyst was fully washed with deionized water and dried in vacuum. For comparison, Pd supported on graphene without nitrogen doping (denoted as Pd/rGO) was prepared by the same process with GO as the support precursor. The specifications of supported Pd catalysts including Pd loadings are summarized in Supporting Information, Table S1.

2.2 Characterization

Scanning electron microscopy (SEM) measurements were carried out on a field emission scanning electron microanalyzer (JEOL-6700F). Nitrogen adsorption-desorption were recorded at $-196 \text{ }^\circ\text{C}$ on a Micromeritics ASAP 2020 analyzer with pretreatment of samples at $150 \text{ }^\circ\text{C}$ for 4 h. Raman spectra were recorded on a Raman spectrometer (LabRAM HR EvoLution) with the green line of an Ar-ion laser of 532 nm. X-ray photoelectron spectroscopy (XPS) were recorded on a RBD upgraded PHI-5000C ESCA system (Perkin Elmer) with Mg or Al $K\alpha$ radiation. Elemental analysis was measured on a PerkinElmer EA2400 II instrument to determine the C, N, and H content of the samples. Transmission electron microscopy (TEM) and energy dispersive X-ray spectroscopy (EDS) measurements were performed using a JEOL JEM-2100 high resolution transmission electron microscope. X-ray diffraction (XRD) patterns were measured on a D/max 2500 PC X-ray diffractometer using Cu $K\alpha$ radiation with a scanning range of 5 – 60 ° . Pd dispersion measurements were conducted using a JAPAN BELCAT Analyzer using a pulsed technique of hydrogen chemisorptions at $50 \text{ }^\circ\text{C}$.

2.3 Catalytic test

The catalytic performances were tested in the hydrogenation of cyclohexene. Typically, 0.01 g catalyst, 0.5–2 mL cyclohexene, and 10 mL ethanol were added into a stainless steel autoclave. After replacing the air in the autoclave with argon, 1 MPa H_2 was injected, and the catalytic tests were then performed at $30 \text{ }^\circ\text{C}$ for 1 h. The products were analyzed by GC (SP-6890) with a OV-101 capillary column. The recovered catalyst was washed with ethanol and employed in the next run.

3. Results and discussion

3.1 Characterization of various catalysts

3.1.1 SEM

As shown in Fig. 1, GO gave large sheets with numerous wrinkles. When GO was hydrothermally treated in different aqueous solutions of above nitrogen sources, three-dimensional porous network with dozens of nanometers pores were obtained. The structures were relatively uniform for various N-doped graphene samples with 3.7 mmol of N-inputting amount. It can be speculated that the three-dimensional microstructures can avoid the stacking of graphene sheets which is a difficult problem for the application of graphene in heterogeneous catalysis. Pd/NG-AW-2.2 gave the similar topological structure to that of Pd/NG-AW-3.7, while different result was obtained on Pd/NG-Urea-2.2. For the SEM image of Pd/NG-Urea-2.2, part of graphene sheets had not been reconstructed, and still maintained the original stacking state. The possible explanation is that the much low concentration of urea ($2.8 \times 10^{-2} \text{ mol} \cdot \text{L}^{-1}$, Table S1 in Supporting Information) for the preparation of Pd/NG-Urea-2.2 restricts the speed or degree of N-doping.

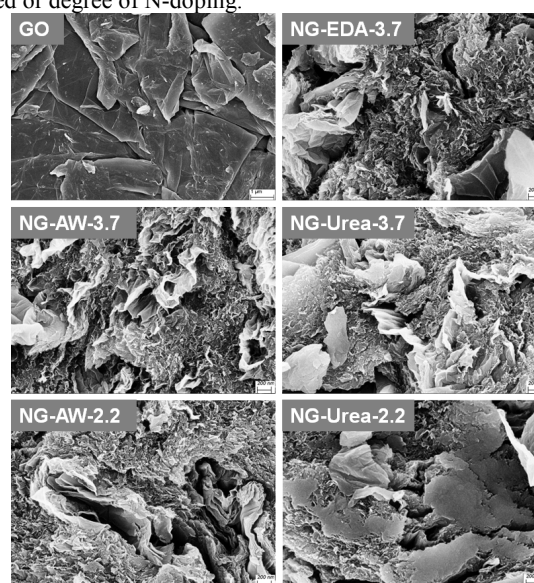


Fig. 1 SEM images of GO and various nitrogen-doped graphene samples.

3.1.2 N_2 adsorption-desorption

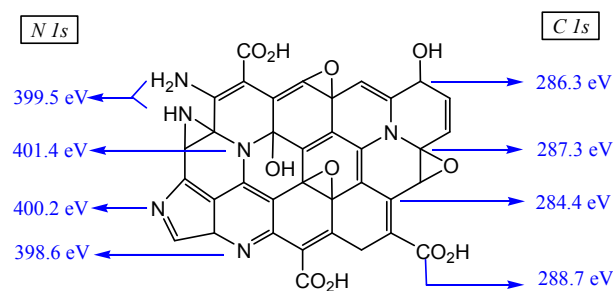
In the results of nitrogen adsorption-desorption measurement (Table 1), GO exhibited a low BET surface area of $87 \text{ m}^2 \cdot \text{g}^{-1}$ with scarcely any pore volume. It is possible that GO sheets got stacking when the water was removed during the pretreatment under vacuum and $150 \text{ }^\circ\text{C}$. Both high BET surface areas and pore volumes for N-doped graphene samples were received, owing to the three-dimensional porous network. It further illustrates that the three-dimensional microstructures of N-doped graphenes are enough stability under the conditions of pretreatment. Comparing different N-doped samples, NG-Urea-3.7 showed the highest BET surface area ($608 \text{ m}^2 \cdot \text{g}^{-1}$) and pore volume ($402 \text{ mm}^3 \cdot \text{g}^{-1}$).

Table 1 BET surface areas and pore volumes for various samples.

Samples	BET surface area/ $(\text{m}^2 \cdot \text{g}^{-1})$	Pore volume / $(\text{mm}^3 \cdot \text{g}^{-1})$
GO	87	—
NG-EDA-3.7	414	268
NG-AW-3.7	429	308
NG-Urea-3.7	608	402

3.1.3 XPS and elemental analysis

As shown in Fig. 2, the spectra reveal that the main chemical components were C 1s, N 1s, O 1s in NG-Urea-3.7, with a clear N 1s peaks around a binding energy of 400 eV. The amount of nitrogen incorporated in NG-Urea-3.7 was found to be 4.6 at%, indicating successful N-doping. The C 1s spectra of GO and NG-Urea-3.7 were separated into four peaks (Fig. 2), at around 284.4, 286.3, 287.3 and 288.7 eV, corresponding to C-C, C-OH, C-O-C and O=C-O groups, respectively (Scheme 1).²⁷ For the result of XPS, GO contained abundant oxygen-containing groups, while much few oxide functionalities were observed on NG-Urea-3.7. Moreover, the N 1s spectrum of NG-Urea-3.7 was also separated into four peaks, at 398.6, 399.5, 400.2, and 401.4 eV. These peaks were successively ascribed to pyridinic N, amine moieties (e.g., -NH- and -NH₂), pyrrolic N, and graphitic N species (Scheme 1).²⁵ Other NG samples (NG-EDA-3.7, NG-AW-2.2 and NG-AW-3.7) showed similar XPS spectra to that of NG-Urea-3.7 (Supporting Information, Fig. S1). It implied that drastic reduction of GO occurred during the hydrothermal treatment, whilst four kinds of nitrogen were doped into the graphene structure.



Scheme 1 A possible structure of NG. The data correspond to the binding energies as obtained from the C and N 1s spectra.

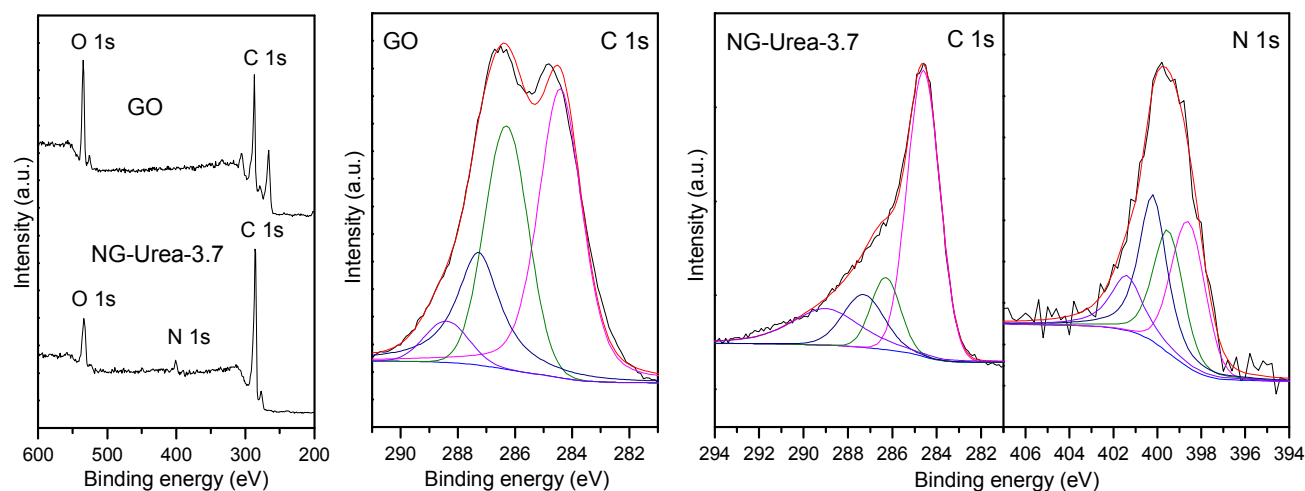


Fig. 2 XPS survey scan and XPS C and N 1s spectra for GO and NG-Urea-3.7.

According to the reported N-doping mechanism in the literatures,^{25,30} the possible N-doping reaction pathway is discussed as follows. When the graphene oxide (GO) is treated under hydrothermal condition, the nitrogen source (ethylenediamine, ammonia, and urea) will react with carboxylic

The chemical composition (contents of C, O, and N) of GO and various N-doped graphene samples with detailed amounts of different nitrogen species obtained by XPS analysis were displayed in Table 2. Compared to the contents of C, O and N obtained by the elemental analysis (Supporting Information, Table S2), O and N amounts decreased, while C amount increased for the results of XPS. It is possible that some C pollution on the surface of samples influence the XPS analysis. Nevertheless, the general tendencies of N-doping situation were consistent for the two results of XPS and elemental analysis. Through hydrothermal treatment in the aqueous solution of ethylenediamine, ammonia, or urea, different nitrogen species and contents were doped into the framework of graphene. Among these N-doped graphenes, NG-EDA-3.7 had the most amounts of nitrogen (6.8 at%); NG-Urea-3.7 and NG-AW-2.2 had similar contents of nitrogen (4.6 and 4.7 at%, respectively) which is slightly lower than that in NG-AW-3.7 (4.9 at%). For the different nitrogen species, relatively more amine moieties (2.1 at%) were observed in NG-EDA-3.7, while less amine moieties (0.9 at%) were included in NG-AW-2.2. NG-Urea-3.7 gave a much less amounts of Graphitic N (0.6 at%). As we all known, different nitrogen species show different behaviors. For the four kinds of nitrogen, pyridinic N and graphitic N are considered to be responsible for stabilizing the metal nanoparticles.^{28,29} In this work, NG-EDA-3.7 possessed the most total amount of pyridinic N and graphitic N, while NG-Urea-3.7 had the least amount. In addition, compared to the oxygen amount of 42.6 at% for GO, less than 30 at% of oxygen were obtained on all N-doped graphenes. It is because that the parts of oxygen-containing functional groups are removed during the N-doping process (Fig. 2). In comparison, NG-Urea-3.7 exhibited the most content of oxygen (23.7 at%), while NG-EDA-3.7 gave the least amount of oxygen (17.3 at%).

acid species on GO to form the amide-like structure. The amide-like structure will convert to the stable aromatic structure or imine by decarbonylation. During this process, GO is reduced simultaneously due to the reaction between nitrogen source and other oxygen-containing groups. Then, the reduced graphene

oxide sheets will assemble into three-dimensional porous network (SEM results) with the π - π interaction.³¹ Moreover, the amine

moieties on the graphene sheets will hinder their stacking by the forming of hydrogen bond.

Table 2 Chemical composition of GO and various N-doped graphenes.

Sample	C/O/N (at%)	Pyridinic N (at%)	Amine moieties (at%)	Pyrrolic N (at%)	Graphitic N (at%)
GO	56.4/42.6/—	—	—	—	—
NG-EDA-3.7	74.9/17.3/6.8	1.7	2.1	1.7	1.3
NG-AW-2.2	73.6/20.2/4.7	1.5	0.9	1.2	1.1
NG-AW-3.7	73.4/19.7/4.9	1.2	1.3	1.4	1.0
NG-Urea-3.7	69.5/23.7/4.6	1.4	1.1	1.5	0.6

Contents of C, O and N and contents of different N kinds were obtained by the XPS analysis.

3.1.4 Raman

As shown in Fig. 3, two main peaks were obtained for all Raman spectra of GO and N-doped graphenes, corresponding to a disorder-induced D band and a sp^2 hybridized G band at about 1350 and 1585 cm^{-1} , respectively.³² When nitrogen elements were introduced into the framework of graphene, I_D/I_G had more or less increase. It indicates that more defect sites form on the graphene sheets or the size of the sp^2 hybridized carbon atom clusters reduces during the process. Significantly, the I_D/I_G decreased gradually with the increase of N-doping contents (Table 1). NG-EDA-3.7 with the most nitrogen amounts showed the lowest I_D/I_G ratio of 1.03, while NG-AW-2.2 gave the highest I_D/I_G ratio of 1.25. It implies that, with increasing the N-introducing contents, more sp^2 hybridized carbon atoms are recovered along with the chemical reduction of GO during the hydrothermal treatment.

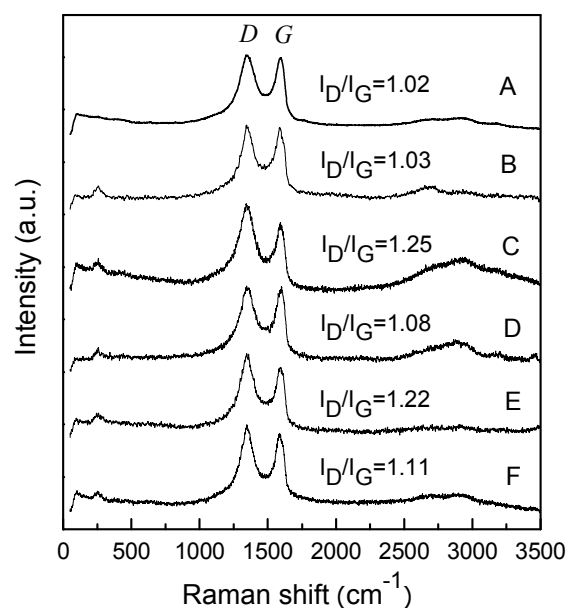


Fig. 3 Raman spectra of GO (A) and nitrogen-doped graphene samples (B-F). (B) NG-EDA-3.7; (C) NG-AW-2.2; (D) NG-AW-3.7; (E) NG-Urea-3.7; (F) NG-Urea-5.2. I_D/I_G : the intensity ratio of D and G band.

3.1.5 TEM

Under the same preparation conditions, large Pd particles with dozens of nanometers were observed for Pd/rGO, while much

smaller Pd particles were obtained on various N-doped graphenes (Fig. 4). The results were consistent with the Pd dispersions shown in Table S3 (Supporting Information). Pd/rGO showed a much low Pd dispersion of 12.1% due to the serious aggregation. Pd supported NG catalysts all gave much higher Pd dispersions beyond 60%. Obviously, nitrogen introducing greatly promotes the dispersion of Pd depending on the increased surface area (Table 1) and nitrogen species (Table 1). It is considered to be that some electron transfer and coordination between Pd and N-doped graphene can prevent the metal from migrating and aggregating.^{33,34} During the Pd/NG catalysts treated with different nitrogen sources, urea-treating samples including Pd/NG-Urea-2.2 and Pd/NG-Urea-3.7 both showed uniform and well-dispersed Pd nanoparticles (NPs). Uneven Pd NPs distributions with some aggregations were exhibited on the NG supports treated with ethylenediamine and ammonia. In comparison, Pd/NG-Urea-3.7 showed the ultrasmall Pd particles with about 2 nm (Fig. 4 F), while Pd/NG-EDA-3.7 gave the relatively large size of Pd particles with 10–12 nm (Fig. 4 B). Combining with the results of elemental analysis and Raman, it can be speculated that the oxygen functional groups and defect sites on the graphene also play important roles in the dispersion of Pd NPs. Compared to Pd/NG-EDA-3.7, despite with less amounts of pyridinic N and graphitic N, Pd/NG-Urea-3.7 gave a higher dispersion of Pd NPs owing to more oxygen groups (Table 2) and defect sites (Fig. 3).

3.1.6 XRD

As shown in Fig. 5, a distinct diffraction peak at 11.4° was observed on GO assigned to the (001) plane of graphene oxide, indicating the successful oxidation of graphite.³⁵ After hydrothermal treatment with urea at 180 °C, the characteristic peak at 11.4° disappeared and new peaks at 24.8° (assigned to the (002) plane of graphite) appeared for NG-Urea-3.7 and Pd/NG-Urea-3.7 (JCPDS card no. 41-1487). It suggests that GO was reduced during the N-doping process. Moreover, Pd/NG-Urea-3.7 showed a low and broad diffraction peak at 39.7°, assigning to the (111) plane of Pd (JCPDS card no. 65-2867).

For the EDS results of NG-Urea-3.7 and Pd/NG-Urea-3.7 (Supporting Information, Fig. S2), C and O elements existed in NG-Urea-3.7, and additional Pd element existed in Pd/NG-Urea-3.7. The peak of N element is overlapped by C peak because of much nearing between the two elements peaks and the strong peak of C element.

Cite this: DOI: 10.1039/c0xx00000x

www.rsc.org/xxxxxx

ARTICLE TYPE

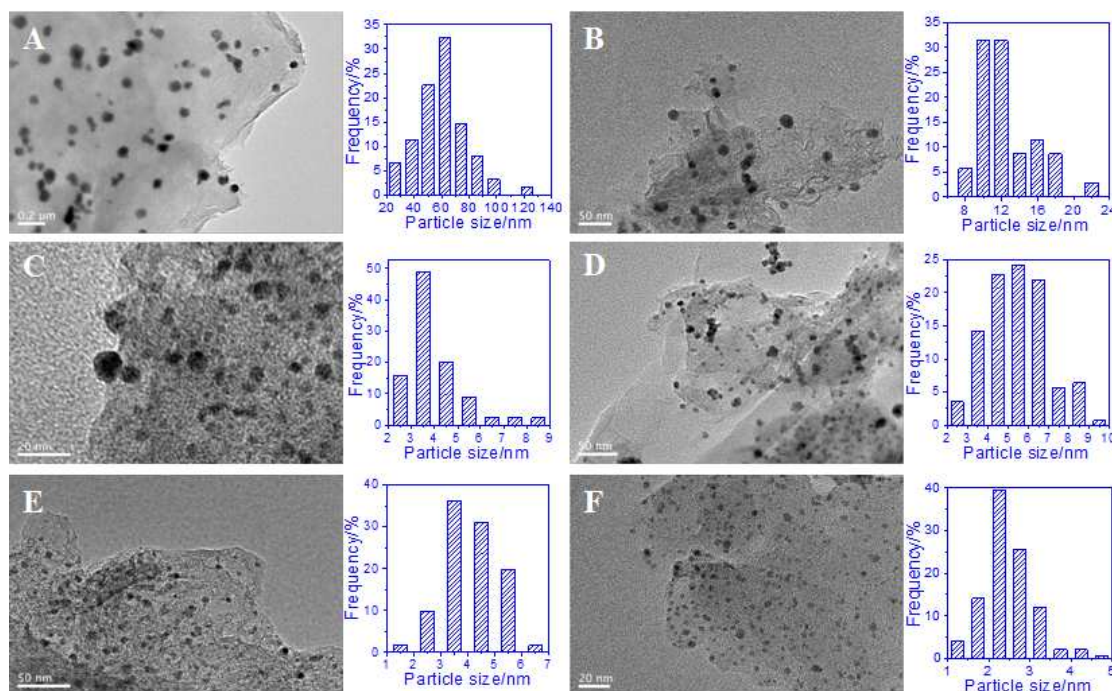


Fig. 4 TEM images and Pd particle size distributions of various Pd-loaded catalysts. (A) Pd/rGO; (B) Pd/NG-EDA-3.7; (C) Pd/NG-AW-2.2; (D) Pd/NG-AW-3.7; (E) Pd/NG-Urea-2.2; (F) Pd/NG-Urea-3.7.

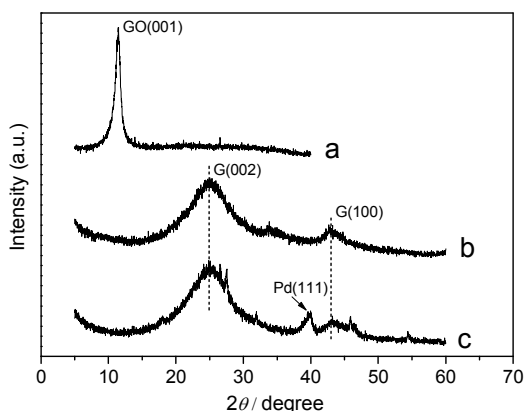


Fig. 5 XRD patterns of GO (a), NG-Urea-3.7 (b), and Pd/NG-Urea-3.7 (c).

3.2 Catalytic studies

3.2.1 Catalytic performances

The hydrogenation of cyclohexene was chosen as the probe reaction to test the catalytic performances of various catalysts because of its simple product. As listed in Table 3, 100% of selectivity to cyclohexane was obtained under the mild reaction conditions over all catalysts without ring-opening, isomerization, or other products. Pd/rGO showed a low conversion of 19.0% with only $1718 \text{ mol} \cdot (\text{mol}_{\text{Pd}} \cdot \text{h})^{-1}$ of TOF under 1.5 MPa, 50 °C

and 1 h. Much low activities were obtained over various NG samples including NG-EDA-3.7, NG-AW-3.7, and NG-Urea-3.7. It suggests that N-doped graphene cannot act as the effective active center for the catalytic hydrogenation of cyclohexene under these reaction conditions. Nevertheless, the activity was significantly improved when N-doped graphenes were employed to support Pd catalysts. Among these Pd/NG catalysts with the same nitrogen inputting amount, Pd/NG-EDA-3.7 exhibited a relatively low activity of 58.2% at 50 °C, while Pd/NG-AW-3.7 and Pd/NG-Urea-3.7 gave a complete transformation of cyclohexene. When the reaction temperature was reduced to 30 °C, 61.0% of conversion with $6530 \text{ mol} \cdot (\text{mol}_{\text{Pd}} \cdot \text{h})^{-1}$ of TOF was obtained over Pd/NG-AW-3.7. For Pd/NG-Urea-3.7, four times of the substrate (2 mL cyclohexene) was employed to make the reaction at the kinetically controlled step. At this case, a 58.9% of conversion with an extremely high TOF of $27463 \text{ mol} \cdot (\text{mol}_{\text{Pd}} \cdot \text{h})^{-1}$ was achieved at 30 °C. Catalytic hydrogenation activities of supported Pd catalysts greatly depend on the dispersion state of Pd NPs. Actually, the dispersion state of Pd determines the number of exposed activity centers. From the results of TEM and Pd dispersion measurement, it can be confirmed that there are much less activity centers on Pd/rGO and more activity centers on Pd/NG catalysts. Therefore, the low TOF of Pd/rGO is because of the agglomeration of Pd particles, and the enhanced activities of various Pd/NG catalysts are precisely attributed to the promoted dispersion of Pd NPs after N-doping

(Fig. 4). During these N-doped catalysts, the superior Pd dispersion of 90.1% with much high density of active sites for Pd/NG-Urea-3.7 leads to the excellent catalytic activity.

Table 3 Comparison of catalytic activities of Pd/NG catalysts in the hydrogenation of cyclohexene.

Catalyst	H ₂ pressure (MPa)	Reaction temperature (°C)	Conversion (%)	Selectivity (%)	TOF ^a (mol·(mol _{Pd} ·h) ⁻¹)
Pd/rGO	1.5	50	19.0	100	1718
NG-EDA-3.7	1.0	50	3.1	100	—
NG-AW-3.7	1.0	50	5.3	100	—
NG-Urea-3.7	1.0	50	4.8	100	—
Pd/NG-EDA-3.7	1.0	50	58.2	100	5871
Pd/NG-AW-3.7	1.0	50	100	100	>10705
Pd/NG-AW-3.7	1.0	30	61.0	100	6530
Pd/NG-Urea-3.7	1.0	50	100	100	>11657
Pd/NG-Urea-3.7 ^b	1.0	30	58.9	100	27463

^a Reaction conditions: 0.01 g catalyst, 0.5 mL cyclohexene, 10 mL ethanol, 1 h.

^b Moles of cyclohexene converted per mole of Pd per hour; ^c 2 mL cyclohexene.

3.2.2 Effect of N-inputting amount

The structural morphology, elemental content of graphene, and the Pd dispersion are all changed during N-doping process (Section 3.1). The above aspects of a catalyst may greatly influence its catalytic performance. Therefore, in order to get a high activity, an appropriate N-doping amount is required. As shown in Fig. 6, 2.2 and 3.7 mmol are the optimum N-inputting amounts for Pd/NG-AW and Pd/NG-Urea, respectively. About 100% conversion of cyclohexene over the two corresponding catalysts were obtained at 30 °C. Comparing the actual contents of N element for NG with different N-doping conditions in Tables 2 and S4 (Supporting Information), with the increase of N-inputting amount, the actual N-doping content increased and oxygen-containing groups reduced gradually. For different N species, there were unified change rule with the increase of N-inputting amount. During the NG-AW and NG-Urea samples, NG-AW-2.2 and NG-Urea-5.2 had the most amounts of Pyridinic N and Graphitic N, respectively. The catalytic activity is closely related with the dispersion state of Pd which depends on several factors, such as N species, oxygen-containing groups, and defect sites on graphene sheets. Considering all the factors, in general, too little or too much N-inputting amount all result in low catalytic activities. Too little nitrogen amount would be not enough to stable the Pd NPs (Tables 2 and S4), while too much nitrogen amount would lead to less defect sites (Fig. 3) and oxygen-containing groups (Tables 2 and S4) which have some contributions to the dispersion of metal (Fig. 4).³⁶ In this work, more amounts of Pyridinic N and Graphitic N for NG-AW-2.2 and more amounts of oxygen-containing groups and defect sites for NG-Urea-3.7 maybe the main reasons for the higher Pd dispersions and superior catalytic activities over their corresponding catalysts. In order to further filtrate the highly efficient catalyst between Pd/NG-AW-2.2 and Pd/NG-Urea-3.7, hydrogenation reaction was carried out at 20 °C. Obviously, Pd/NG-Urea-3.7 showed a superior conversion of 83.7% to that of 27.5% for Pd/NG-AW-2.2.

3.2.3 Catalytic recycling

The catalytic recycling of Pd/NG-Urea-3.7 was carried out at 30 °C and 1.0 MPa, shown in Fig. 7. It can be seen that Pd/NG-Urea-3.7 can be reused for at least five times with no obvious reduction of the catalytic activity. The TOFs were always over 26000 mol·(mol_{Pd}·h)⁻¹, indicating good stability for the catalyst

of Pd-supported on N-doped graphene in heterogeneous hydrogenation system.

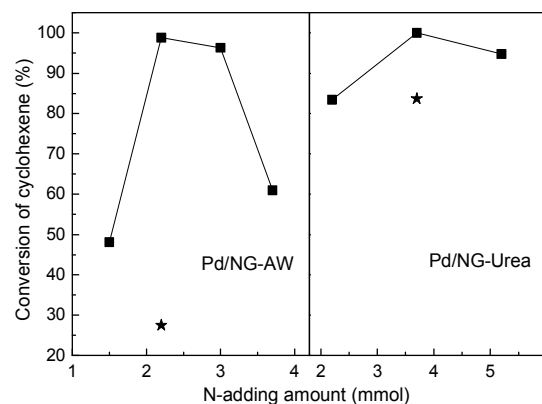


Fig. 6 The conversion of cyclohexene over Pd/NG-AW and Pd/NG-Urea with different N-adding amount. Reaction conditions: 0.01 g catalyst, 0.5 mL cyclohexene, 10 mL ethanol, 30 °C, 1.0 MPa, 1 h. ★ stands for the conversion of cyclohexene at 20 °C.

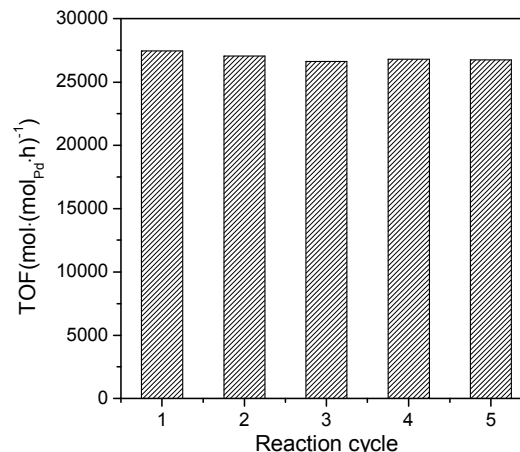


Fig. 7 Turnover frequency in different catalytic cycles of Pd/NG-Urea-3.7 in the hydrogenation of cyclohexene. Reaction conditions: 0.01 g catalyst, 0.5 mL cyclohexene, 10 mL ethanol, 30 °C, 1.0 MPa, 1 h.

3.2.4 Substrate expansion

The hydrogenations of different olefins over Pd/NG-Urea-3.7 were performed at the same reaction conditions, and the results

were showed in Table 4. Generally, aliphatic olefins including 1-hexene and 1-heptene had much low conversions, while styrene had the highest conversion. The transformation rates of cycloolefins (cyclopentene and cyclohexene) were in the middle level. 36602 mol·(mol_{Pd}·h)⁻¹ of TOF was obtained in the hydrogenation of styrene, more than three times to those of the hydrogenation of aliphatic olefins. The ultrahigh TOF is possibly attributed to the π-electron interaction between graphene and the benzene ring of styrene, which promotes the adsorption of styrene on the graphene sheets. In addition, the comparison of catalytic activities of Pd/NG-Urea-3.7 with the commercial Pd/C in the hydrogenation of cyclohexene was made (Supporting Information, Table S5). At 30 °C, 1 MPa H₂ pressure, a more than two times of catalytic activity was obtained over Pd/NG-Urea-3.7 than that over the commercial Pd/C. It demonstrates that the N-doped graphene with urea is a perfect carrier for Pd particles for catalyzing the hydrogenation of olefins.

Table 4 Results of the hydrogenation of different olefins over the Pd/NG-Urea-3.7 catalyst.

Reactant	Conversion (%)	Selectivity (%)	TOF (mol·(mol _{Pd} ·h) ⁻¹)
1-hexene	23.9	100	11144
1-heptene	20.1	100	9372
cyclopentene	52.6	100	24526
cyclohexene	58.9	100	27463
styrene	78.5	100	36602

Reaction conditions: 0.01 catalyst, 2 mL reactant, 10 mL ethanol, 30 °C, 1 h, 1 MPa H₂ pressure.

4. Conclusions

Enhanced hydrogenation activities with highly dispersed Pd NPs were obtained on N-doped graphenes synthesized by hydrothermal treatment at a mild condition. Among various Pd/NG catalysts with different nitrogen sources and adding amounts, Pd/NG-Urea-3.7 exhibited the highest catalytic hydrogenation activity, along with good stability. The high surface area, as well as more defect sites and oxygen-containing groups for the NG-Urea-3.7, significantly promoted the dispersion of Pd NPs, and further improved the catalytic activity.

Acknowledgments

The authors thank the National Natural Science Foundation of China (Nos. 21406019 and 21376032), the Natural Science Foundation of Jiangsu Province (No. BK20130250), the Natural Science Foundation of the Jiangsu Higher Education Institutions (No. 13KJB530001), the Jiangsu Key Laboratory of Advanced Catalytic Materials and Technology (No. BM2012110), the State Key Laboratory of Materials-Oriented Chemical Engineering (No. KL14-12) and the Priority Academic Program Development of Jiangsu Higher Education Institutions for financial support.

Notes and references

^a Address, Jiangsu Key Laboratory of Advanced Catalytic Materials and Technology, College of Chemistry and Chemical Engineering, Changzhou University, Gehu Road 1, Changzhou, Jiangsu 213164, PR China. Fax: +86-519-86330135; Tel: +86-519-86330135; E-mail: pingliu02@163.com (Ping Liu); liyxluck@163.com (Yong-Xin Li)

^b State Key Laboratory of Materials-oriented Chemical Engineering, College of Chemistry and Chemical Engineering, Nanjing University of Technology, Nanjing 210009, China

- J.J. Martinez, E. Nope, H. Rojas, M.H. Brijaldo, F. Passos and G. Romanelli, *J. Mol. Catal. A-Chem.*, 2014, **392**, 235.
- G. Wu, X. Wang, N. Guan and L. Li, *Appl. Catal. B: Environ.*, 2013, **136-137**, 177.
- N. Li, J. Du, L. Xu, J. Xu and T. Chen, *Chem. Eng. J.*, 2014, **240**, 161.
- H. Yuan, C. Zhang and W. Huo, *J. Chem. Sci.*, 2014, **126**, 141.
- Y. Zhao, *Environ. Chem. Lett.*, 2014, **12**, 185.
- A.A. Kurokhtina, E.V. Larina, A.F. Schmidt, A. Malaika, B. Krzyzyska, P. Rechnia and M. Kozlowski, *J. Mol. Catal. A-Chem.*, 2013, **379**, 327.
- S.C. Qi, X.Y. Wei, Z.M. Zong and Y.K. Wang, *RSC Adv.*, 2013, **3**, 14219.
- C.M.A. Parlett, P. Keshwalla, S.G. Wainwright, D.W. Bruce, N.S. Hondow, K. Wilson and A.F. Lee, *ACS Catal.*, 2013, **3**, 2122.
- S. Ohara, Y. Hatakeyama, M. Umetsu, Z.Q. Tan and T. Adschiri, *Adv. Powder Technol.*, 2011, **22**, 559.
- M. Fattahi, M. Kazemini, F. Khorasheh and A. Rashidi, *Chem. Eng. J.*, 2014, **250**, 14.
- L.H. Hess, A. Lyuleeva, B.M. Blaschke, M. Sachsenhauser, M. Seifert, J.A. Garrido and F. Deubel, *ACS Appl. Mater. Inter.*, 2014, **6**, 9705.
- Z. Wang, C. Xu and G. Gao, *RSC Adv.*, 2014, **4**, 13644.
- A. Bragaru, E. Vasile, C. Obreja, M. Kusko, M. Danila and A. Radoi, *Mater. Chem. Phys.*, 2014, **146**, 538.
- Q. Zhao, D. Chen, Y. Li, G. Zhang, F. Zhang and X. Fan, *Nanoscale*, 2013, **5**, 882.
- Y. Li, X.B. Fan, J.J. Qi, J.Y. Ji, S.L. Wang, G.L. Zhang and F.B. Zhang, *Mater. Res. Bull.*, 2010, **45**, 1413.
- S. Zhang, Y. Shao, H. Liao, J. Liu, I.A. Aksay, G. Yin and Y. Lin, *Chem. Mater.*, 2011, **23**, 1079.
- P. Wu, Y. Huang, L. Zhou, Y. Wang, Y. Bu and J. Yao, *Electrochim. Acta*, 2015, **152**, 68.
- B. Choi, H. Yoon, I.-S. Park, J. Jang and Y.-E. Sung, *Carbon*, 2007, **45**, 2496.
- P. Chen, L. M. Chew, A. Kostka, M. Muhler and W. Xia, *Catal. Sci. Technol.*, 2013, **3**, 1964.
- J. Zhang, L. Ma, M. Gan, F. Yang, S. Fu and X. Li, *J. Power Sources*, 2015, **288**, 42.
- X.K. Kong, Z.Y. Sun, M. Chen, C.L. Chen and Q.W. Chen, *Energ. Environ. Sci.*, 2013, **6**, 3260.
- A.A. Koos, A.T. Murdock, P. Nemes-Incze, R.J. Nicholls, A.J. Pollard, S.J. Spencer, A.G. Shard, D. Roy, L.P. Biro and N. Grobert, *Phys. Chem. Chem. Phys.*, 2014, **16**, 19446.
- X. Wang, X. Li, L. Zhang, Y. Yoon, P.K. Weber, H. Wang, J. Guo and H. Dai, *Science*, 2009, **324**, 768.
- X. Chen, D.P. He and S.C. Mu, *Prog. Chem.*, 2013, **25**, 1292.
- P. Chen, T.Y. Xiao, H.H. Li, J.J. Yang, Z. Wang, H.B. Yao and S.H. Yu, *Nano Energy*, 2013, **2**, 249.
- W.S. Hummers and R.E. Offeman, *J. Am. Chem. Soc.*, 1958, **80**, 1339.
- Y. Xu, H. Bai, G. Lu, C. Li and G. Shi, *J. Am. Chem. Soc.*, 2008, **130**, 5856.
- R. Arrigo, M. E. Schuster, Z. Xie, Y.Yi, G. Wowsnick, L. L. Sun, K. E. Hermann, M. Friedrich, P. Kast, M. Hävecker, A. Knop-Gericke and R. Schlögl, *ACS Catal.*, 2015, **5**, 2740.
- X. Ning, H. Yu, F. Peng and H. Wang, *J. Catal.*, 2015, **325**, 136.
- R. Arrigo, M. Hävecker, S. Wrabetz, R. Blume, M. Lerch, J. McGregor, E. P. J. Parrott, J. A. Zeitler, L. F. Gladden, A. Knop-Gericke, R. Schlögl and D. S. Su, *J. Am. Chem. Soc.*, 2010, **132**, 9616.
- Y. X. Xu, K. X. Sheng, C. Li and G. Q. Shi, *Acs Nano*, 2010, **4**, 4324.
- Z. Rong, Z. Sun, Y. Wang, J. Lv and Y. Wang, *Catal. Lett.*, 2014, **144**, 980.
- L. S. Ott and R. G. Finke, *Coord. Chem. Rev.*, 2007, **251**, 1075.
- Z. Li, J. Liu, C. Xia and F. Li, *ACS Catal.*, 2013, **3**, 2440.
- Z. Lv, X. Yang and E. Wang, *Nanoscale*, 2013, **5**, 663.
- G. Goncalves, P.A.A.P. Marques, C.M. Granadeiro, H.I.S. Nogueira, M.K. Singh and J. Gracio, *Chem. Mater.*, 2009, **21**, 4796.